



HAL
open science

Considerations on higher-order finite elements for multilayered plates based on a unified formulation

M. d'Ottavio, D. Ballhause, T. Wallmersperger, B. Kröplin

► **To cite this version:**

M. d'Ottavio, D. Ballhause, T. Wallmersperger, B. Kröplin. Considerations on higher-order finite elements for multilayered plates based on a unified formulation. *Computers & Structures*, 2006, 84 (19-20), pp.1222-1235. hal-01367082

HAL Id: hal-01367082

<https://hal.science/hal-01367082>

Submitted on 10 Jan 2019

HAL is a multi-disciplinary open access archive for the deposit and dissemination of scientific research documents, whether they are published or not. The documents may come from teaching and research institutions in France or abroad, or from public or private research centers.

L'archive ouverte pluridisciplinaire **HAL**, est destinée au dépôt et à la diffusion de documents scientifiques de niveau recherche, publiés ou non, émanant des établissements d'enseignement et de recherche français ou étrangers, des laboratoires publics ou privés.

Considerations on higher-order finite elements for multilayered plates based on a Unified Formulation

M. D'Ottavio, D. Ballhause, T. Wallmersperger, B. Kröplin

1. Introduction

One of the most challenging tasks in modern engineering sciences is to design and implement highly efficient structural components enabling to save weight and, at the same time, to improve mechanical characteristics, like the stiffness or the damage tolerance. A predominant role is played in this context by multilayered structures, in which different materials are laminated in order to tailor the global properties in a desired manner. In this field, fiber-reinforced materials have gained the main attention due to their intrinsic anisotropy and lightweight. Thin multilayered components, like plates and shells, have been the object of intensive research since many decades, particularly in aerospace engineering. A very large amount of two-dimen-

sional models for the design and simulation of laminated plates and shells built up from fiber-reinforced materials have been proposed. Accordingly, many review articles have been devoted to this subject, among them the early contribution of Ambartsumyan [1], the exhaustive article of Noor and Burton [2] and the recent review of Carrera [3].

Relevant phenomena occurring in multilayered composites require the formulation of accurate models for an adequate design simulation: even global response characteristics can in fact be strongly influenced by localized phenomena occurring at smaller scales, see, e.g., Librescu [4]. An accurate determination of the local stress state is mandatory for meaningful design or verification analyses involving for example damage and failure mechanisms. Kant and Swaminathan have given an overview of different techniques to estimate the transverse stresses in laminated composites [5]. Among them, post-processing steps, e.g., a direct integration of the three-dimensional equilibrium equations, are often performed in combination with

* Corresponding author. Tel.: +49 711 68562484; fax: +49 711 68563706.

E-mail address: dottavio@isd.uni-stuttgart.de (M. D'Ottavio).

simpler computational models like the classical laminate theory (see, e.g., [6]). However, this procedure does not allow to account for the interlaminar equilibrium within the governing equations of the problem. Furthermore, the discontinuous slopes of the displacements at the layers' interfaces should be modeled for an accurate response of the laminate. Both conditions have been summarized as the “ C_z^0 -Requirements” an accurate model for laminates should be able to fulfill [7]. Additionally, the role of transverse normal stresses should be particularly mentioned: the inclusion of this component affords in fact a distribution of the transverse shear stresses in thickness direction, thus allowing the consistent satisfaction of homogeneous stress boundary conditions on the outer surfaces of the shell. The relevance of the transverse normal stress has been recognized e.g. for curved shells [8], for thermally loaded laminates [9] and for locally loaded sandwich components [10].

Many different approaches fulfilling fully or partly the C_z^0 -Requirements have been proposed, involving formulations based either on displacements-based variational statements, or on mixed principles; these latter have both displacements and stresses as primary unknowns. Formulations basing on a partial mixed theorem formulated by Reissner [11] have proven to give excellent results [12,13]. Following Reddy [14], axiomatically derived two-dimensional models can be further divided in “Equivalent Single Layer” and “Layerwise” classes: while in the former description method the unknowns are independent from the number of layers, the latter involves layer-specific unknowns. A series of these axiomatic approaches has been uniformly derived by Carrera [15] upon developing a so-called “Unified Formulation” for the general description of two-dimensional formulations for multilayered plates and shells. With the Unified Formulation it is possible to implement in a single software a series of hierarchic formulations, thus affording a systematic assessment of different theories, ranging from simple ESL models up to higher-order layerwise descriptions. This formulation is a valuable tool for gaining a deep insight in the complex mechanics of laminated structures.

The two-dimensional problem, which arises once the thickness assumptions have been introduced, can be solved in different manners. For some limited geometries, lay-ups and boundary/loading conditions, a closed-form, Navier-type solution may be found. For the analysis of more complex and realistic structural problems, the finite element method (FEM) can be considered as the established technique. Many multilayered finite plate and shell elements have been proposed basing on classical laminate theory as well as on first- and higher-order shear deformation theories, see, e.g., [16]. The severe numerical problems experienced by early shear-deformable theories in the thin plate limits could be successfully circumvented by the use of numerical tricks, like the reduced/selective quadrature techniques with adequate hourglass controls; a different approach involves more systematically derived mecha-

nisms, like the mixed interpolation of tensorial components (MITC-elements) proposed by Bathe and Dvorkin [17] or the enhanced assumed strain methods (EAS-elements) introduced by Simo and Rifai [18]. First-order shear deformation elements including the transverse normal strain and the fully three-dimensional material law are often prone to the spurious *thickness locking* due to the Poisson effect. There are several viable techniques to circumvent this effect: a modification of the constitutive equations, see, e.g., [19,20]; a refinement of the transverse normal strains by the introduction of either an additional assumed transverse strain component [21] or a higher-order thickness assumption for the transverse deflection, as for example in the work of Parisch [22]. A survey of the numerical issues associated to the in-plane and the transverse behavior of shell elements can be found in the article of Yang et al. [23].

Unified Formulation-based finite elements have been already implemented and successfully verified [24]. Nonetheless, a more thorough analysis of the numerical properties of this class of elements is still lacking. Particularly, the question of the performance of the elements for thin structures shall be addressed. More general, the influence of higher-order thickness assumptions, involving transverse shear and transverse normal stresses, on the in-plane behavior of the finite element discretization shall be analyzed. Once these questions obtain a satisfactory answer, the Unified Formulation may become a very useful tool for systematically deriving accurate multilayered finite plate and shell elements.

An outline of the paper is as follows: Section 2 introduces the employed notation for the geometry and the kinematic as well as for the constitutive behavior of the laminated plate; Section 3 is dedicated to the axiomatic modeling and presents the Unified Formulation. The definition and assembly of the finite element matrices, and the numerical assessment of the resulting formulations are reported in Sections 4 and 5, respectively. Some considerations on the thickness locking phenomenon associated to Unified Formulation-based elements are presented at the end of Section 5.

2. Preliminaries

The multilayered plate considered in this work is depicted in Fig. 1. It consists of N_l layers which are considered to be perfectly bonded. Ω indicates the reference surface of the laminated plate. The reference surface is defined by the two coordinate axes x and y . z denotes the coordinate in thickness direction and has its origin on Ω . Local coordinates are introduced in each layer: the local reference surface Ω_k is placed in the middle of each layer k at a distance z_{0_k} from the laminate reference surface. z_k is the local thickness coordinate and ranges from $-h_k/2$ to $+h_k/2$. A correspondent dimensionless coordinate $\zeta_k = 2z_k/h_k$, being h_k the thickness of the k th layer, is introduced ranging from -1 to 1 .

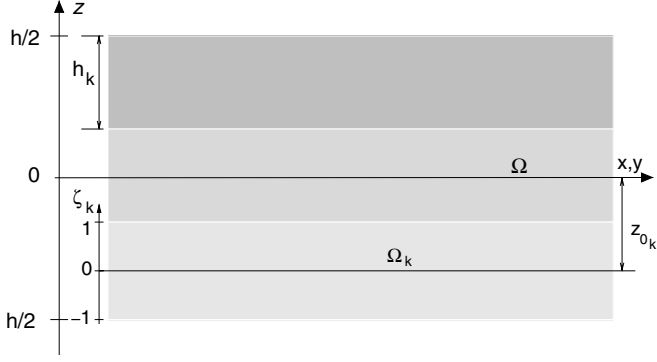


Fig. 1. Geometry and notations introduced for the description of a multilayered plate.

2.1. Variational statement

The governing equations are derived within the principle of virtual displacements (PVD). The complete statement of the principle reads [25]

$$\int_V \sigma_q^T \delta \epsilon_q dV - \int_V f_i^T \delta u_i dV - \int_{\Gamma_t} \bar{t}_i^T \delta u_i d\Gamma = 0 \quad (1)$$

The index i runs from 1 to 3, q from 1 to 6; for the stress and strain tensors of second order the contracted notation according to $1 = xx, 2 = yy, 3 = zz, 4 = yz, 5 = xz, 6 = xy$ has been used. In the remainder of this paper, the three spatial axes will be interchangeably denoted as $\langle x, y, z \rangle, \langle 1, 2, 3 \rangle$ or $\langle x_1, x_2, x_3 \rangle$ without confusion. f_i and t_i are the vectors of the body forces and of the surface tractions, respectively; V is the whole domain and Γ_t is the portion of boundary on which the mechanical tractions are applied. Within the theory of small displacements, the strains ϵ_{ij} are related to the displacements by the geometric relations

$$\epsilon_{ij} = \frac{1}{2} (\partial_i u_j + \partial_j u_i) \quad i, j = 1, 2, 3 \quad (2)$$

where the notation ∂_i indicates the partial derivation with respect to the coordinate x_i , i.e. $\partial_i = \partial / \partial x_i$. A representation within the contracted vector notation of the geometric relations equation (2) is introduced according to

$$\epsilon_q = D_{qi} u_i \quad (3)$$

where D_{qi} is the 6×3 differential operator defined by Eq. (2).

For the sake of completeness, it is here recalled that the PVD satisfies in a weak sense the equilibrium equations in the domain V

$$\partial_j \sigma_{ij} + f_i = 0 \quad i, j = 1, 2, 3 \quad (4)$$

as well as the mechanical boundary conditions on Γ_t

$$\sigma_{ij} l_j = \bar{t}_i \quad i, j = 1, 2, 3 \quad (5)$$

On the other hand, the PVD has as subsidiary conditions both the geometric relations equation (2) and the boundary conditions for the prescribed displacements given on the portion Γ_u ($\Gamma = \Gamma_u \cup \Gamma_t$):

$$u_i = \bar{u}_i \quad i = 1, 2, 3 \quad (6)$$

2.2. Constitutive equations

The PVD holds in the form given in Eq. (1) irrespective of the material stress strain relations. These relations are given within the linear elasticity theory for each layer k of the multilayered plate according to Hooke's law

$$\sigma_q^k = \tilde{C}_{qr}^k \epsilon_r^k \quad q, r = 1, 2, \dots, 6 \quad (7)$$

where the previously introduced contracted notation has been employed. Substitution of the geometric relations equation (3) in the material law equation (7), and upon introduction of the resulting expressions of the stresses in terms of displacements into Eq. (1), the PVD is written for the multilayered structure as

$$\sum_{k=1}^{N_l} \left[\int_{V^k} \left(C_{qr}^k D_{rj} u_j^k \right)^T (D_{qi} \delta u_i^k) dV - \int_{V^k} (f_i^k)^T \delta u_i^k dV - \int_{\Gamma_t^k} (\bar{t}_i^k)^T \delta u_i^k d\Gamma \right] = 0 \quad (8)$$

3. Two-dimensional modeling of multilayered plates

In all two-dimensional axiomatic models of plates and shells, the key point is represented by the assumptions made for the behavior in the thickness direction: this allows to eliminate the dependencies on the thickness coordinate and to obtain a set of differential equations for the behavior in the reference surface Ω of the structure. In view to this different treatment of the thickness (i.e. *transverse*) direction and of the *in-plane* directions, the strain and stress vectors ϵ_q and σ_q are split into their in-plane (subscript p) and transverse (subscript n) components

$$(\epsilon_p)_i^k = [\epsilon_1^k \epsilon_2^k \epsilon_6^k]^T; \quad (\sigma_p)_i^k = [\sigma_1^k \sigma_2^k \sigma_6^k]^T$$

$$(\epsilon_n)_i^k = [\epsilon_4^k \epsilon_5^k \epsilon_3^k]^T; \quad (\sigma_n)_i^k = [\sigma_4^k \sigma_5^k \sigma_3^k]^T$$

Accordingly, the geometric relations (3) read

$$(\epsilon_p)_i^k = (D_p)_{ij} u_j^k \quad (9a)$$

$$(\epsilon_n)_i^k = (D_{n\Omega})_{ij} u_j^k + (D_{nz})_{ij} u_j^k \quad (9b)$$

where the following layer-independent differential operators have been introduced:

$$(D_p)_{ij} = \begin{bmatrix} \partial_x & 0 & 0 \\ 0 & \partial_y & 0 \\ \partial_y & \partial_x & 0 \end{bmatrix}; \quad (D_{n\Omega})_{ij} = \begin{bmatrix} 0 & 0 & \partial_x \\ 0 & 0 & \partial_y \\ 0 & 0 & 0 \end{bmatrix};$$

$$(D_{nz})_{ij} = \begin{bmatrix} \partial_z & 0 & 0 \\ 0 & \partial_z & 0 \\ 0 & 0 & \partial_z \end{bmatrix} \quad (10)$$

Hooke's law (7) is split analogously reading

$$(\sigma_p)_i^k = (\tilde{C}_{pp})_{ij}^k (\epsilon_p)_j^k + (\tilde{C}_{pn})_{ij}^k (\epsilon_n)_j^k \quad (11a)$$

$$(\sigma_n)_i^k = (\tilde{C}_{np})_{ij}^k (\epsilon_p)_j^k + (\tilde{C}_{nn})_{ij}^k (\epsilon_n)_j^k \quad (11b)$$

where the stiffness matrices for a monoclinic material are considered:

$$(\tilde{C}_{pp})_{ij}^k = \begin{bmatrix} \tilde{C}_{11} & \tilde{C}_{12} & \tilde{C}_{16} \\ \tilde{C}_{12} & \tilde{C}_{22} & \tilde{C}_{26} \\ \tilde{C}_{16} & \tilde{C}_{26} & \tilde{C}_{66} \end{bmatrix}; \quad (\tilde{C}_{pm})_{ij}^k = \begin{bmatrix} 0 & 0 & \tilde{C}_{13} \\ 0 & 0 & \tilde{C}_{23} \\ 0 & 0 & \tilde{C}_{36} \end{bmatrix} \quad (12a)$$

$$(\tilde{C}_{np})_{ij}^k = \begin{bmatrix} 0 & 0 & 0 \\ 0 & 0 & 0 \\ \tilde{C}_{13} & \tilde{C}_{23} & \tilde{C}_{36} \end{bmatrix}; \quad (\tilde{C}_{mm})_{ij}^k = \begin{bmatrix} \tilde{C}_{44} & \tilde{C}_{45} & 0 \\ \tilde{C}_{45} & \tilde{C}_{55} & 0 \\ 0 & 0 & \tilde{C}_{33} \end{bmatrix} \quad (12b)$$

The relation between the stiffness coefficients \tilde{C}_{qr} and the elasticity parameters E_i , G_{ij} and ν_{ij} can be found, e.g., in the reference work of Jones [26]. Note that Eqs. (7) and (11b) are constitutive equations written in the structure reference frame, i.e. the stiffness coefficients \tilde{C}_{qr} already include the information concerning the angle between the material axes and the structure reference system. Finally, the PVD equation (8) can be rewritten as

$$\begin{aligned} \sum_{k=1}^{N_l} \left[\int_{V^k} [(D_p)_{li} \delta u_i^k]^T (\tilde{C}_{pp})_{lm}^k [(D_p)_{mj}] u_j^k \right. \\ + [(D_p)_{li} \delta u_i^k]^T (\tilde{C}_{pm})_{lm}^k [(D_{n\Omega})_{mj} + (D_{nz})_{mj}] u_j^k \\ + [((D_{n\Omega})_{li} + (D_{nz})_{li}) \delta u_i^k]^T (\tilde{C}_{np})_{lm}^k [(D_p)_{mj}] u_j^k \\ + [((D_{n\Omega})_{li} + (D_{nz})_{li}) \delta u_i^k]^T (\tilde{C}_{nn})_{lm}^k [(D_{n\Omega})_{mj} + (D_{nz})_{mj}] u_j^k dV \\ \left. - \int_{V^k} (f_i^k)^T \delta u_i^k dV - \int_{\Gamma_i^k} (\bar{t}_i^k)^T \delta u_i^k d\Gamma \right] = 0 \quad (13) \end{aligned}$$

Once the general framework has been given, in the next sections the assumptions for the behavior in thickness direction and the technique for solving the resulting two-dimensional problem are presented.

3.1. Thickness assumptions: the Unified Formulation

This work relies on the Unified Formulation (UF) summarised in [15]. By an extensive use of index notations, the UF is a useful tool to easily implement a large number of two-dimensional models. Starting point is the description at layer level of all the governing and subsidiary equations derived above. As usual in axiomatic modeling, the thickness distributions of the unknowns and of the weighting functions, i.e. the displacements u_j^k and their virtual variations δu_i^k , respectively, are expressed in terms of known functions $F(z_k)$

$$u_j^k(x, y, z) = F_s(z_k) (\hat{u}_j(x, y))_s^k \quad (14a)$$

$$\delta u_i^k(x, y, z) = F_\tau(z_k) (\delta \hat{u}_i(x, y))_\tau^k \quad (14b)$$

τ and s are summation indices ranging from 0 to N , where N is the order of the expansion assumed for the through-thickness behavior. While τ is employed for the virtual variations, s is used for the expansion of the unknowns.

By varying the free parameter N , a *hierarchical* series of two-dimensional models is obtained: more refined models are attained by increasing the expansion order N . Without loss of generality, throughout this work both unknowns and weighting functions are treated with the same order of expansion. Additionally, all displacement components are described with the same expansion in thickness direction as well. This means that even first-order expansions naturally include the effects of transverse normal strains and stress in the analysis. Classical formulations neglecting these effects, like the established classical laminate theory (CLT) or the first-order shear deformation theory (FSDT), may be recovered by means of standard penalty techniques.

Since the thickness assumptions are made for each layer, the known functions F are generally defined in the local, layer-specific coordinate z_k . The assumed functions $F(z_k)$ are chosen depending on the desired model. The behavior of the complete laminate is finally obtained by assembling in the proper way the contributions of all layers.

3.1.1. Layerwise models

Within a layerwise (LW) – or discrete-layer – model, each layer has its own unknowns, and the whole laminate is described by a number of unknowns which depends on the number of layers. The layer-specific unknowns, i.e. the displacements of the layer, must be assembled to the multilayered level by respecting the condition of perfectly bonded interfaces. In order to enforce the interlaminar continuity (IC) of the displacements at the layers' interfaces, the interpolating functions F are conveniently chosen as combinations of Legendre polynomials $P(\zeta_k)$ (see [27] for more details)

$$F_t^k(z_k) = \frac{P_0(\zeta_k) + P_1(\zeta_k)}{2}; \quad F_b^k(z_k) = \frac{P_0(\zeta_k) - P_1(\zeta_k)}{2} \quad (15a)$$

$$F_\tau^k(z_k) = P_\tau - P_{\tau-2} \quad \text{with } \tau = 2, 3, \dots, N \quad (15b)$$

Due to these interpolation functions, the unknowns associated to the linear expansion for $N = 1$ represent the values of the unknowns at the top (F_t) and bottom (F_b) of the layer. Additional nodes along the z_k -axis introduce a higher-order distribution of the unknowns in the layer thickness. The IC conditions are hereafter enforced by setting

$$(\hat{u}_j)_{\tau=t}^k = (\hat{u}_j)_{\tau=b}^{k+1} \quad (16)$$

Throughout this work, models based on a layerwise description of the displacements will be denoted by the acronym LDN; therefore, an LD1 formulation assumes in each layer a linear behavior of the displacements in thickness direction, an LD2 model has a quadratic layerwise distribution and so on. Fig. 2(a) exemplarily depicts a distribution of displacements in thickness direction which can be represented by a layerwise second-order expansion.

3.1.2. Equivalent single layer models

If a number of total unknowns is desired which is independent from the number of layers constituting the

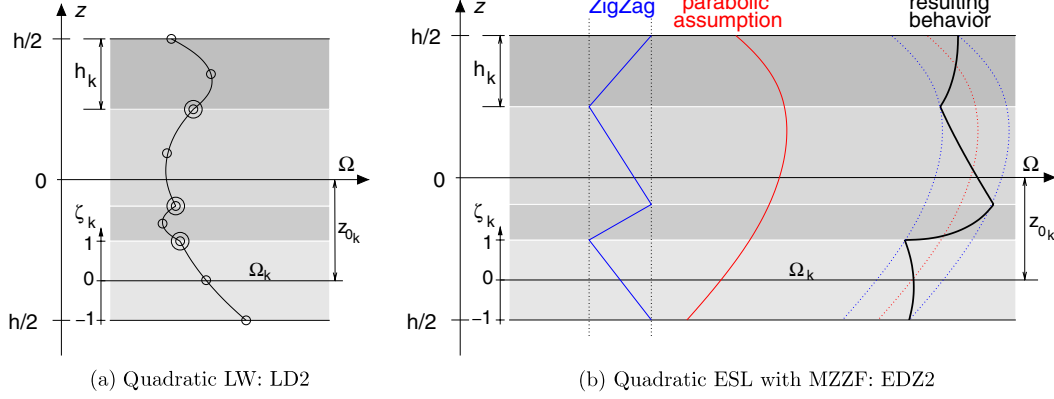


Fig. 2. Examples for possible models within the Unified Formulation: layerwise (left) and equivalent single layer with ZigZag (right).

laminate, an equivalent single layer (ESL) description is addressed. Usually, a Taylor expansion is used according to

$$F_{\tau}^k(z_k) = (z_k)^{\tau} \quad \text{with } \tau = 0, 1, \dots, N-1 \quad (17)$$

In this case, the unknowns related to $\tau = 0$ are simply the values on the reference surface of the laminate. Here, the displacement unknowns associated with $\tau = 1$ represent the rotations of the cross-section in an analogous way compared to FSDT.

A refinement of ESL formulations can be achieved by superimposing to the above expansion the so-called Murakami ZigZag function (MZZF), first introduced by Murakami [28] and extensively employed by Carrera [29]. This function allows the introduction of a discontinuity in the slopes of the displacements and thus represents a step towards the fulfillment of the C_z^0 -Requirements. In this latter case, the expansion equation (17) is extended by the ZigZag term yielding the following through-thickness approach

$$u_j^k(x, y, z_k) = (z_k)^{\tau} \left(\hat{u}_j^k(x, y) \right)_{\tau} + (-1)^k \zeta_k^{\tau} (\hat{u}_j^k(x, y))_{ZZ} \quad (18)$$

The typical behavior of an approach obtained with Eq. (18) is depicted in Fig. 2(a). It is important to underline that the MZZF introduces a dependency of the through-thickness behavior on the layer number within a layer-independent ESL formulation. Nonetheless, the added unknown $(\hat{u}_j^k(x, y))_{ZZ}$ assumes the same value for each layer, thus respecting the layer-independency of the basis formulation.

Formulations based on a ESL description are denoted as EDN models; if the MZZF is superimposed to the ED-formulation, the model will be indicated as EDZN.

3.2. Finite element approximation

According to the well established finite element technique, the infinite number of degrees of freedom of a flexible structure is reduced to a finite number of nodal unknowns. For a detailed description of the FEM, reference is made to the large number of available publications

and books on this topic. In this work, standard isoparametric lagrangian elements are employed.

The expression of the displacement field given in Eq. (14b) is discretized within the FE approach as

$$u_j^k(x, y, z) = N_r(x, y) F_s(z_k) (\hat{U}_j)_{sr}^k \quad (19a)$$

$$\delta u_i^k(x, y, z) = N_q(x, y) F_{\tau}(z_k) (\delta \hat{U}_i)_{\tau q}^k \quad (19b)$$

where the shape functions N_r ($r = 1, 2, \dots, N_n$ for an element with N_n nodes) have been introduced and are responsible for the in-plane behavior of the displacement field. An analogous expression holds for the virtual variations of the displacements δu_i^k . Within ESL formulations, the shape functions are naturally defined on the reference surface Ω for the laminated plate. For LW descriptions, the same shape functions are employed for all layers. $(\hat{U}_j)_{rs}^k$ and $(\delta \hat{U}_i)_{\tau q}^k$ are the vectors of the nodal displacements and of their virtual variations, respectively. The previously introduced indices are summarized for clarity:

- i, j indicate the components of the displacement and range from 1 to 3 (spatial directions);
- k is the layer index, ranging from 1 to the number of layers N_l ;
- τ, s denote the expansion in thickness direction and range from 0 to the maximum order N ;
- q, r indicate the node numbers within the finite element approximation ranging from 1 to the number of element nodes N_n .

4. Finite element matrices

For a given value of the indices k, τ, s, q and r , upon introduction of the expressions in Eq. (19) into the PVD equation (13), the governing equations are expressed in terms of a 3×3 array called the *fundamental nucleus* of the formulation. For a pure displacement-based variational form, the fundamental nucleus consists of a single 3×3 array. In case of multifield mixed formulations, the fundamental arrays are more than one, see for example the description within the UF based upon Reissner mixed

variational theorem (RMVT) [30]. The key point of the UF consists expressly in the capability to represent a large number of formulations by the simple building of these fundamental arrays. The fundamental nuclei obtained for different values of the indices are then assembled in order to obtain the governing equations for the whole structure.

4.1. The fundamental nucleus

Starting point for the derivation of the fundamental nucleus is the variational equation (13): introduction in the expression for the internal work in the PVD of both the through-thickness assumptions and the finite element interpolations equation (19) yields

$$\begin{aligned} \int_{V^k} \left((\delta \widehat{U}_i)_{\tau q}^k \right)^T & [(D_p)_{li} N_q F_\tau]^T (\widetilde{C}_{pp})_{lm}^k [(D_p)_{mj} N_r F_s] (\widehat{U}_j)_{sr}^k \\ & + \left((\delta \widehat{U}_i)_{\tau q}^k \right)^T [(D_p)_{li} N_q F_\tau]^T (\widetilde{C}_{pm})_{lm}^k [(D_{n\Omega})_{mj} \\ & + (D_{nz})_{mj} N_r F_s] (\widehat{U}_j)_{sr}^k + \left((\delta \widehat{U}_i)_{\tau q}^k \right)^T [(D_{n\Omega})_{li} \\ & + (D_{nz})_{li} N_q F_\tau]^T (\widetilde{C}_{np})_{lm}^k [(D_p)_{mj} N_r F_s] (\widehat{U}_j)_{sr}^k \\ & + \left((\delta \widehat{U}_i)_{\tau q}^k \right)^T [(D_{n\Omega})_{li} + (D_{nz})_{li} N_q F_\tau]^T (\widetilde{C}_{nm})_{lm}^k [(D_{n\Omega})_{mj} \\ & + (D_{nz})_{mj} N_r F_s] (\widehat{U}_j)_{sr}^k dV = \delta L_{\text{ext}}^k - \delta L_{\text{int}}^k \end{aligned} \quad (20)$$

The virtual internal and external works read, respectively

$$\delta L_{\text{int}}^k = - \int_{V^k} (f_i^k)^T \delta u_i^k dV; \quad \delta L_{\text{ext}}^k = \int_{\Gamma_i^k} (\bar{t}_i^k)^T \delta u_i^k d\Gamma \quad (21)$$

The dimension of the above array is defined by the variation of the free indices i, j , i.e. the three spatial directions x, y, z . The differential operators quoted in Eq. (10) act either on the in-plane functions $N(x, y)$ or on the thickness interpolations $F(z_k)$. Upon splitting the whole domain V^k in the reference surface Ω^k and the thickness A^k , and separated the terms related to the thickness behavior from those related to the in-plane behavior, the PVD finally reads

$$\left((\delta \widehat{U}_i)_{\tau q}^k \right)^T (K_{ij})_{q\tau sr}^k (\widehat{U}_j)_{sr}^k = \delta L_{\text{ext}}^k - \delta L_{\text{int}}^k \quad (22)$$

with the fundamental nucleus $(K_{ij})_{q\tau sr}^k$ expressed as

$$\begin{aligned} (K_{ij})_{q\tau sr}^k &= \int_{\Omega^k} ((D_p)_{li} N_q) (\widetilde{C}_{pp})_{lm}^k \left[\int_{A^k} F_\tau F_s dz \right] ((D_p)_{mj} N_r) dx dy \\ &+ \int_{\Omega^k} ((D_p)_{li} N_q) (\widetilde{C}_{pm})_{lm}^k \left[\int_{A^k} F_\tau F_s dz \right] ((D_{n\Omega})_{mj} N_r) dx dy \\ &+ \int_{\Omega^k} ((D_p)_{li} N_q) (\widetilde{C}_{pn})_{lm}^k \left[\int_{A^k} F_\tau F_{s_z} dz \right] N_r dx dy \\ &+ \int_{\Omega^k} ((D_{n\Omega})_{mj} N_q) (\widetilde{C}_{np})_{lm}^k \left[\int_{A^k} F_\tau F_s dz \right] ((D_p)_{mj} N_r) dx dy \\ &+ \int_{\Omega^k} ((D_{n\Omega})_{mj} N_q) (\widetilde{C}_{nm})_{lm}^k \left[\int_{A^k} F_\tau F_s dz \right] ((D_{n\Omega})_{mj} N_r) dx dy \\ &+ \int_{\Omega^k} ((D_{n\Omega})_{mj} N_q) (\widetilde{C}_{nn})_{lm}^k \left[\int_{A^k} F_\tau F_{s_z} dz \right] N_r dx dy \end{aligned}$$

$$\begin{aligned} &+ \int_{\Omega^k} N_q (\widetilde{C}_{np})_{lm}^k \left[\int_{A^k} F_{\tau_z} F_s dz \right] ((D_p)_{mj} N_r) dx dy \\ &+ \int_{\Omega^k} N_q (\widetilde{C}_{nn})_{lm}^k \left[\int_{A^k} F_{\tau_z} F_s dz \right] ((D_{n\Omega})_{mj} N_r) dx dy \\ &+ \int_{\Omega^k} N_q (\widetilde{C}_{nn})_{lm}^k \left[\int_{A^k} F_{\tau_z} F_{s_z} dz \right] N_r dx dy \end{aligned} \quad (23)$$

4.1.1. Numerical quadrature techniques

All integrals appearing in the fundamental nucleus equation (23) are computed with the Gauss quadrature technique. The integrals over the layer thickness are all evaluated in an exact manner. As far as the integration over the surface Ω^k is concerned, three different techniques have been employed:

- the full integration (“normal” integration, referred to as IN scheme) evaluates all terms exactly;
- the classical selectively reduced technique (IS scheme) evaluates exactly the terms related to the normal stresses and the terms related to the in-plane shear stress, whereas the terms related to the transverse shear stresses σ_4 and σ_5 are reduced integrated;
- the “extended selectively reduced” integration (IS2 scheme) integrates in a reduced manner all transverse stress components, i.e. the transverse shear stresses σ_4 and σ_5 and the transverse normal stress σ_3 ; all in-plane stress contributions are exactly integrated.

For a more detailed description of the meaning and background of the first two quadrature techniques (IN and IS) the reader is referred to the FEM-specific literature. The new introduced IS2 quadrature scheme is a simple extension of the selectively reduced integration scheme treating in a consistent manner all transverse stress components [30].

In order to give evidence of the terms affected by the reduced integration schemes, the fundamental nucleus equation (23) is re-written introducing the following notations:

$$\begin{aligned} &\left\{ (Z_{pp}^{k\tau s})_{ij}, (Z_{pn}^{k\tau s})_{ij}, (Z_{np}^{k\tau s})_{ij}, (Z_{nn}^{k\tau s})_{ij} \right\} \\ &= \left\{ (\widetilde{C}_{pp})_{ij}^k, (\widetilde{C}_{pn})_{ij}^k, (\widetilde{C}_{np})_{ij}^k, (\widetilde{C}_{nn})_{ij}^k \right\} E_{\tau s} \end{aligned} \quad (24a)$$

$$\begin{aligned} &\left\{ (Z_{pn}^{k\tau s_z})_{ij}, (Z_{nn}^{k\tau s_z})_{ij}, (Z_{np}^{k\tau s_z})_{ij}, (Z_{nn}^{k\tau s_z})_{ij}, (Z_{nn}^{k\tau s_z})_{ij} \right\} \\ &= \left\{ (\widetilde{C}_{pn})_{ij}^k E_{\tau s_z}, (\widetilde{C}_{nn})_{ij}^k E_{\tau s_z}, (\widetilde{C}_{np})_{ij}^k E_{\tau s_z}, \right. \\ &\quad \left. (\widetilde{C}_{nn})_{ij}^k E_{\tau s_z}, (\widetilde{C}_{nn})_{ij}^k E_{\tau s_z} \right\} \end{aligned} \quad (24b)$$

where the integrals E are defined as

$$\{ E_{\tau s}, E_{\tau s_z}, E_{\tau s_z}, E_{\tau s_z} \} = \int_{A^k} \{ F_\tau F_s, F_{\tau_z} F_s, F_\tau F_{s_z}, F_{\tau_z} F_{s_z} \} dz \quad (24c)$$

With the above introduced quantities, the fundamental nucleus reads

$$(K_{xx})_{q\tau sr}^k = (Z_{pp}^{k\tau s})_{11} \triangleleft N_{q,x} N_{r,x} \triangleright \Omega^k + (Z_{pp}^{k\tau s})_{16} \triangleleft N_{q,y} N_{r,x} \triangleright \Omega^k \\ + (Z_{pp}^{k\tau s})_{16} \triangleleft N_{q,x} N_{r,y} \triangleright \Omega^k + (Z_{pp}^{k\tau s})_{66} \triangleleft N_{q,y} N_{r,y} \triangleright \Omega^k \\ + (Z_{nn}^{k\tau s,z})_{55} \triangleleft N_q N_r \triangleright \Omega^k$$

$$(K_{xy})_{q\tau sr}^k = (Z_{pp}^{k\tau s})_{12} \triangleleft N_{q,x} N_{r,y} \triangleright \Omega^k + (Z_{pp}^{k\tau s})_{26} \triangleleft N_{q,y} N_{r,y} \triangleright \Omega^k \\ + (Z_{pp}^{k\tau s})_{16} \triangleleft N_{q,x} N_{r,x} \triangleright \Omega^k + (Z_{pp}^{k\tau s})_{66} \triangleleft N_{q,y} N_{r,x} \triangleright \Omega^k \\ + (Z_{nn}^{k\tau s,z})_{45} \triangleleft N_q N_r \triangleright \Omega^k$$

$$(K_{xz})_{q\tau sr}^k = (Z_{pn}^{k\tau s,z})_{13} \triangleleft N_{q,x} N_{r,z} \triangleright \Omega^k + (Z_{pn}^{k\tau s,z})_{36} \triangleleft N_{q,y} N_{r,z} \triangleright \Omega^k \\ + (Z_{nn}^{k\tau s,z})_{55} \triangleleft N_q N_{r,x} \triangleright \Omega^k + (Z_{nn}^{k\tau s,z})_{45} \triangleleft N_q N_{r,y} \triangleright \Omega^k$$

$$(K_{yx})_{q\tau sr}^k = (Z_{pp}^{k\tau s})_{12} \triangleleft N_{q,y} N_{r,x} \triangleright \Omega^k + (Z_{pp}^{k\tau s})_{16} \triangleleft N_{q,x} N_{r,x} \triangleright \Omega^k \\ + (Z_{pp}^{k\tau s})_{26} \triangleleft N_{q,y} N_{r,y} \triangleright \Omega^k + (Z_{pp}^{k\tau s})_{66} \triangleleft N_{q,x} N_{r,y} \triangleright \Omega^k \\ + (Z_{nn}^{k\tau s,z})_{45} \triangleleft N_q N_r \triangleright \Omega^k$$

$$(K_{yy})_{q\tau sr}^k = (Z_{pp}^{k\tau s})_{22} \triangleleft N_{q,y} N_{r,y} \triangleright \Omega^k + (Z_{pp}^{k\tau s})_{26} \triangleleft N_{q,x} N_{r,y} \triangleright \Omega^k \\ + (Z_{pp}^{k\tau s})_{26} \triangleleft N_{q,y} N_{r,x} \triangleright \Omega^k + (Z_{pp}^{k\tau s})_{66} \triangleleft N_{q,x} N_{r,x} \triangleright \Omega^k \\ + (Z_{nn}^{k\tau s,z})_{44} \triangleleft N_q N_r \triangleright \Omega^k$$

$$(K_{yz})_{q\tau sr}^k = (Z_{pn}^{k\tau s,z})_{23} \triangleleft N_{q,y} N_{r,z} \triangleright \Omega^k + (Z_{pn}^{k\tau s,z})_{36} \triangleleft N_{q,x} N_{r,z} \triangleright \Omega^k \\ + (Z_{nn}^{k\tau s,z})_{45} \triangleleft N_q N_{r,x} \triangleright \Omega^k + (Z_{nn}^{k\tau s,z})_{44} \triangleleft N_q N_{r,y} \triangleright \Omega^k$$

$$(K_{zx})_{q\tau sr}^k = (Z_{nn}^{k\tau s,z})_{55} \triangleleft N_q N_{r,x} \triangleright \Omega^k + (Z_{nn}^{k\tau s,z})_{45} \triangleleft N_{q,y} N_{r,x} \triangleright \Omega^k \\ + (Z_{np}^{k\tau s,z})_{13} \triangleleft N_q N_{r,x} \triangleright \Omega^k + (Z_{np}^{k\tau s,z})_{36} \triangleleft N_q N_{r,y} \triangleright \Omega^k$$

$$(K_{zy})_{q\tau sr}^k = (Z_{nn}^{k\tau s,z})_{45} \triangleleft N_{q,x} N_{r,y} \triangleright \Omega^k + (Z_{nn}^{k\tau s,z})_{44} \triangleleft N_{q,y} N_{r,y} \triangleright \Omega^k \\ + (Z_{np}^{k\tau s,z})_{23} \triangleleft N_q N_{r,y} \triangleright \Omega^k + (Z_{np}^{k\tau s,z})_{36} \triangleleft N_q N_{r,x} \triangleright \Omega^k$$

$$(K_{zz})_{q\tau sr}^k = (Z_{nn}^{k\tau s,z})_{55} \triangleleft N_{q,x} N_{r,x} \triangleright \Omega^k + (Z_{nn}^{k\tau s,z})_{45} \triangleleft N_{q,y} N_{r,x} \triangleright \Omega^k \\ + (Z_{nn}^{k\tau s,z})_{45} \triangleleft N_{q,x} N_{r,y} \triangleright \Omega^k + (Z_{nn}^{k\tau s,z})_{44} \triangleleft N_{q,y} N_{r,y} \triangleright \Omega^k \\ + (Z_{nn}^{k\tau s,z})_{33} \triangleleft N_q N_r \triangleright \Omega^k$$

The terms marked with a simple box ($\triangleleft \square \triangleright$) are those related to the transverse shear stresses and are reduced integrated within the IS and IS2 scheme. The terms marked with the double box ($\triangleleft \square \square \triangleright$) are related to the transverse normal stresses and are reduced integrated only within the IS2 quadrature technique.

4.2. Assembly of fundamental nuclei

Once the fundamental nucleus for each layer, each couple τ, s and each node pairs q, r has been built, the array has to be assembled to form the structure stiffness. Since the assembly for different nodes is a well-known standard procedure of the FEM, the description of this step is omitted for brevity. We focus on the assembly procedure for different τ, s and, finally, from the layer-specific matrix to the multilayered stiffness. By varying the indices related to the through-thickness expansions τ, s , the original 3×3 fundamental nucleus is expanded to the layer-specific

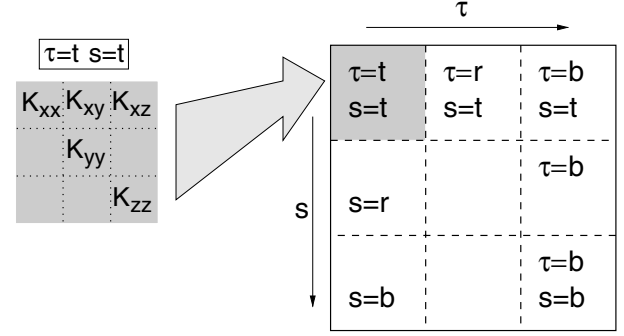
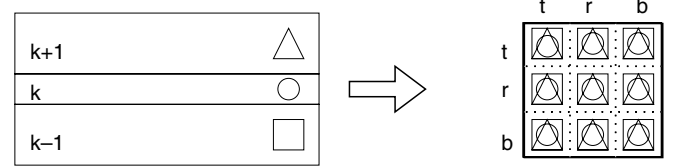
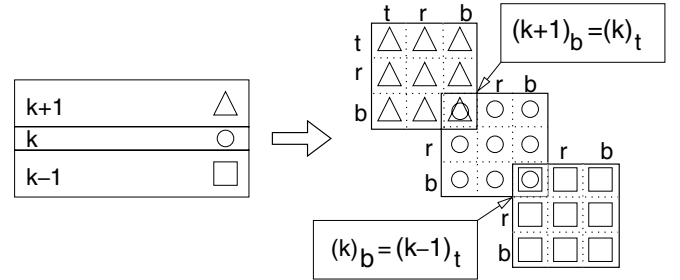


Fig. 3. Expansion of the fundamental nucleus (3×3 -array) to the layer-specific stiffness matrix.



(a) Multilayer assembly for ESL descriptions



(b) Multilayer assembly for LW descriptions

Fig. 4. Schemes for the assembly of multilayered stiffness from layer-specific contributions.

stiffness according to the scheme depicted in Fig. 3. Finally, the multilayer stiffness is assembled from the contributions of the single layers depending on the description method which has been selected. In case of ESL formulations, since all unknowns are defined for the reference surface of the laminated plate, all layers contributions are simply superimposed, see Fig. 4(a). In case of LW descriptions, the layer contributions need to be assembled by fulfilling the interlaminar continuity conditions expressed by Eq. (16); this results in the assembly procedure visualized in Fig. 4(b).

5. Numerical assessment of the FE formulation

An extensive analysis is presented of the convergence properties as well as of the accuracy of the hierarchic formulations for multilayered plates described in the previous sections. A case study has been taken, for which the exact elasticity solution was found by Pagano [31]. Moreover, for

the present case study, analytical solutions have been computed for the various UF-based plate models. This means that same through-thickness assumptions described in Section 3.1 are used, but the resulting two-dimensional problem is analytically solved in closed-form instead of with the FE approximation, see e.g., [32]. Since the analytical solutions base on the same thickness assumptions and no numerical approximation is made in the solution procedure for the resulting two-dimensional model, the FE solution is expected to converge to the values obtained by the closed-form solution. In the following, analytical solutions are denoted by a superscript a .

The selected problem consists of a multilayered, rectangular plate with dimensions a and $b = 3a$ and thickness h , see Fig. 5. The plate is a symmetric, three-ply laminate of graphite/epoxy (Gr/Ep) with the stacking sequence [0/90/0]; all plies have an identical thickness, i.e. $h_1 = h_2 = h_3 = h/3$. The material properties of the plies are given in the table in Fig. 5, where L indicates the fiber direction and T the directions transverse to the fibers. In the outer layers, the fiber orientation is aligned with the x -axis. The plate is considered to be simply-supported on the four edges, i.e.

$$u(y, z) = w(y, z) = 0 \quad \text{at } x = 0, a \quad (25)$$

$$v(x, z) = w(x, z) = 0 \quad \text{at } y = 0, b \quad (26)$$

A bisinusoidal distributed transverse pressure load is applied on the top surface of the plate according to

$$p(x, y) = p_0 \sin\left(\frac{\pi x}{a}\right) \sin\left(\frac{\pi y}{b}\right) \quad \text{at } z = +h/2 \quad (27)$$

In order to obtain comparable data for all considered geometries, the following normalized quantities have been introduced:

$$S = \frac{a}{h} \quad (28a)$$

$$\bar{w} = \frac{100E_T}{p_0hS^4} w\left(\frac{a}{2}, \frac{b}{2}, 0\right) \quad (28b)$$

$$\begin{aligned} & \{\bar{\sigma}_{xx}; \bar{\sigma}_{yy}; \bar{\sigma}_{xy}\} \\ &= \frac{1}{p_0S^2} \left\{ \sigma_{xx}\left(\frac{a}{2}, \frac{b}{2}, \frac{h}{2}\right); \sigma_{yy}\left(\frac{a}{2}, \frac{b}{2}, -\frac{h}{6}\right); \sigma_{xy}\left(0, 0, -\frac{h}{2}\right) \right\} \end{aligned} \quad (28c)$$

$$\{\bar{\sigma}_{xz}; \bar{\sigma}_{yz}\} = \frac{1}{p_0S} \left\{ \sigma_{xz}\left(0, \frac{b}{2}, 0\right); \sigma_{yz}\left(\frac{a}{2}, 0, 0\right) \right\} \quad (28d)$$

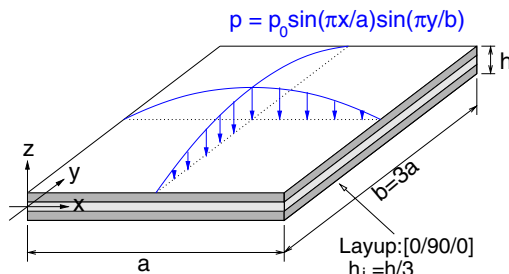


Fig. 5. Geometrical and material properties of the considered case study.

Note that the various CLT solutions are independent from the thickness ratio $1/S$ once the above defined normalized quantities are employed. The transverse shear stresses σ_{xz} and σ_{yz} have been always computed by direct integration of the three-dimensional equilibrium equations (Eq. (4), with $f_i = 0$) in a post-processing step. The in-plane stresses have been computed by Hooke's law. Furthermore, the in-plane stress σ_{yy} has been taken in the central layer because there it reaches its maximum value.

5.1. Numerical properties of "Unified Formulation"-based FE

In the following, some results are presented to show the numerical performance of the proposed FE. The behavior of some selected FE for varying thickness ratio and for a given discretization is depicted in Fig. 6. The most accurate ESL (ED4) and LW (LD4) formulations, as well as the most accurate EDZ (EDZ3) formulation, have been selected; for comparison, the linear LD1 and ED1 formulations are included in the analysis. The three different integration schemes presented in Section 4.1.1 have been considered. The exact elasticity solution of Pagano as well as the CLT solution are given for comparison purposes: for thin plates, the CLT results coincide with the 3D-solution. The selected formulations are seen to recover the elasticity solution over a wide range of thickness ratios. The layer-wise, higher-order formulation (LD4) is capable to capture the exact solution even for very thick plates. Equivalent single layer, lower-order formulations (for example ED1) cannot correctly resolve all thickness effects and are therefore less accurate.

For thin plates (i.e. large S), a typical "locking" phenomenon appears for the full integrated bilinear elements, see Fig. 6(a): the transverse deflection is dramatically underestimated, the plate is said to "lock". The nine-noded quadratic element seems to not suffer this spurious stiffening effect arising at small thickness ratios. Observing the graphics related to the selectively reduced integrated elements (Fig. 6(c)–(f)), it can be stated that the locking phenomenon could be successfully circumvented. Since the IS scheme acts only on the transverse shear terms, and this scheme is sufficient to eliminate the locking phenomenon, it can be concluded that only a *shear locking* is involved in the present elements. Summarizing, only full integrated

E_T	1×10^6 [psi]
E_L/E_T	25
G_{LT}/E_T	0.5
G_{TT}/E_T	0.2
$\nu_{LT} = \nu_{TT}$	0.25 [-]

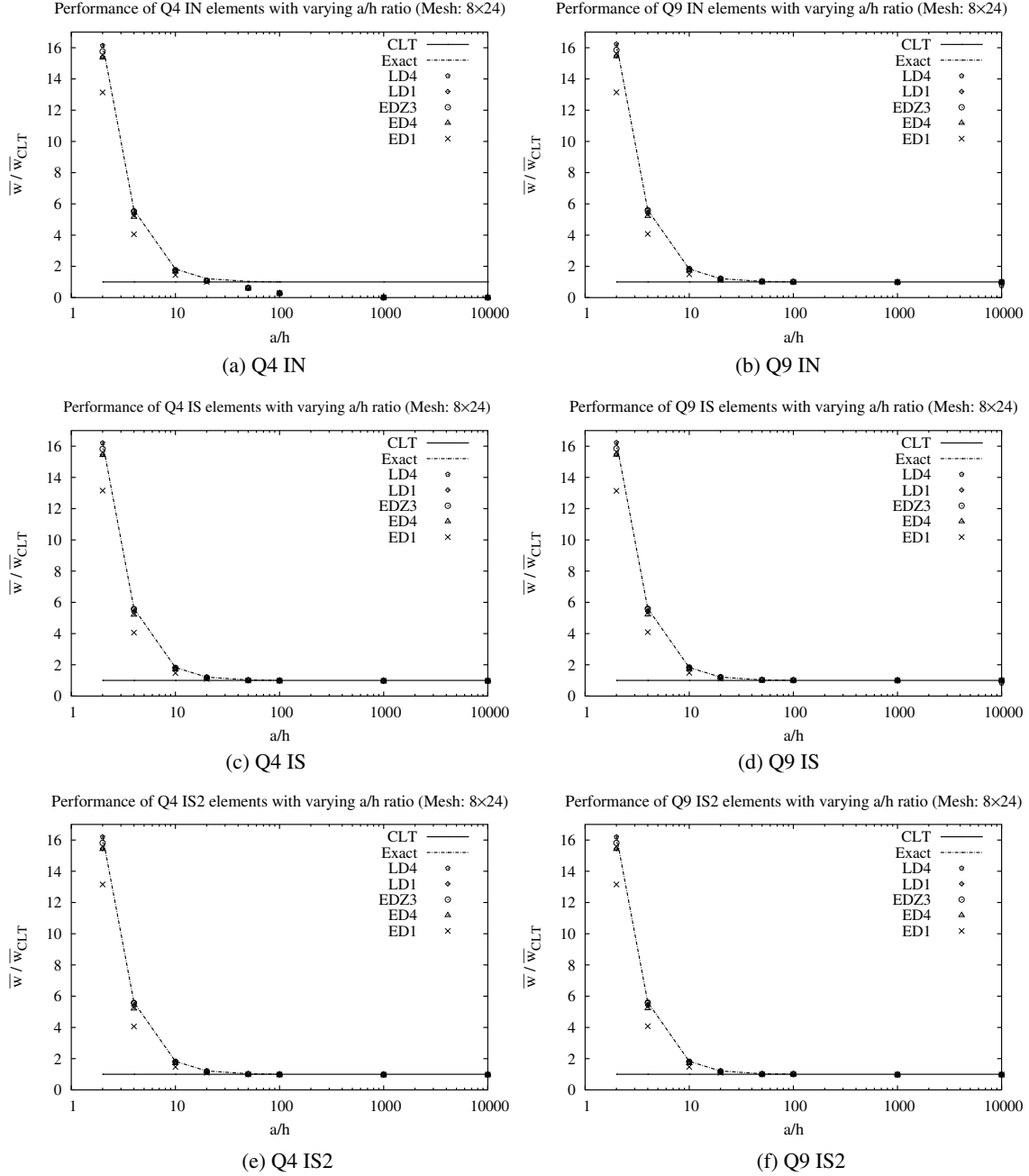


Fig. 6. Performance of the proposed elements for varying thickness ratio: transverse displacement \bar{w} referred to CLT solution \bar{w}_{CLT} (mesh: 8×24).

bilinear elements (Q4, IN) suffer the *shear locking*. Moreover, no complicating numerical effect is seen to be introduced by taking into account the transverse normal stresses or, more generally, higher-order thickness assumptions.

Once the behavior of the present finite elements has been considered for a given discretization at varying thickness ratios, an analysis of the FE solution for varying elements number is presented. The convergence of some selected formulations is depicted in Fig. 7 as a function of the number of total elements used in the discretization. Only quadratic-shaped elements have been employed, this means that the number of elements in y -direction is three times the number

of elements introduced in x -direction. A quadratic convergence for Q9 elements and a linear convergence for Q4 elements could be recovered for a thick plate (Fig. 7(a)) and for a thin plate with reduced integrated elements (Fig. 7(c) and (d)). The difficulties experienced by full integrated elements for a thin plate are well recognizable in Fig. 7(b): in this case, the convergence order of Q9 elements is reduced to approximately 1.5 and the one of Q4 to approximately 0.5. In all cases, the quadratic Q9 elements are more accurate than the bilinear Q4 elements. Once again, the effectiveness of the employed reduced integration schemes is confirmed: for thin plates, the recovery of the original convergence order is achieved by both the IS and

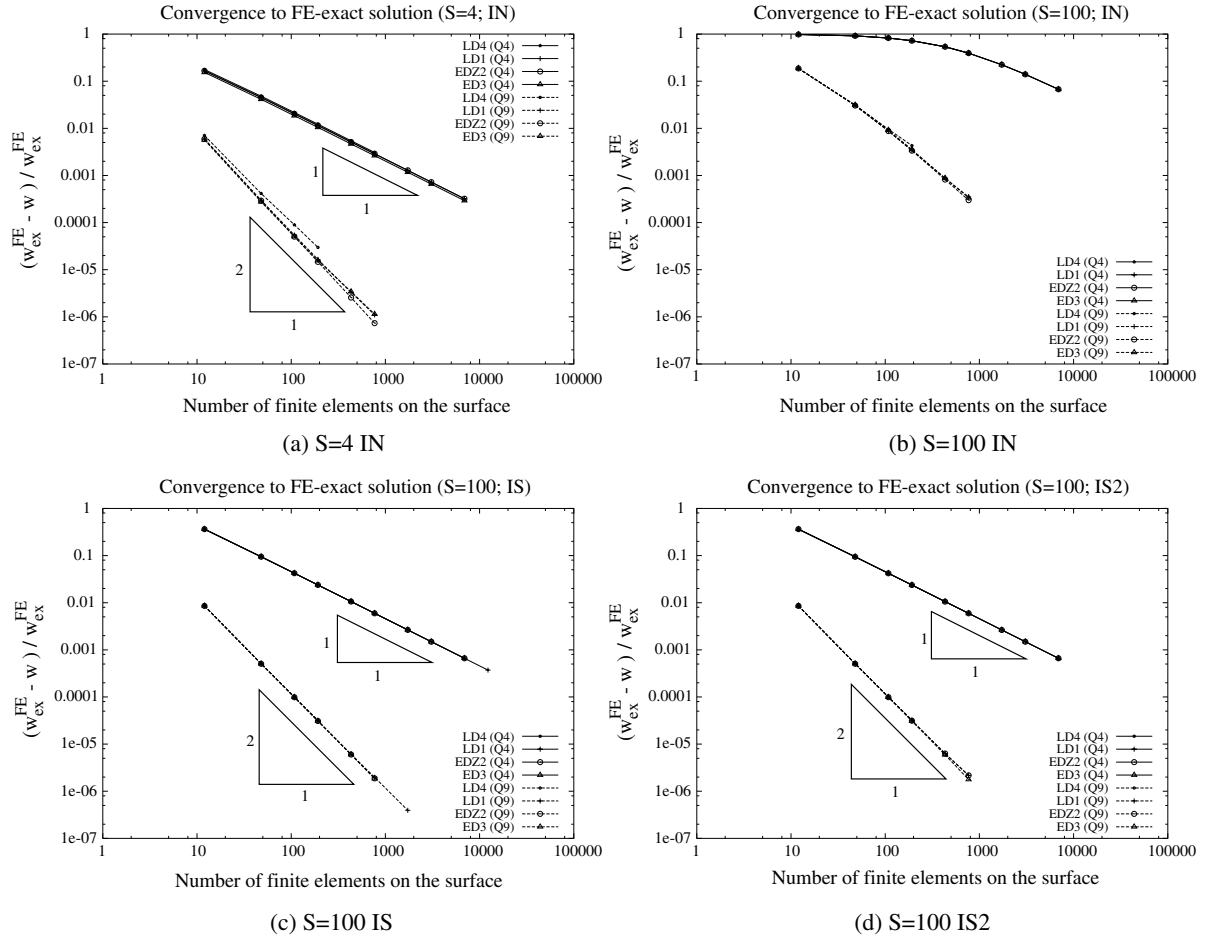


Fig. 7. Convergence analysis: normalized transverse deflection \bar{w} .

IS2 quadrature schemes. The convergence analysis for the in-plane normal stress $\bar{\sigma}_{xx}$ and for the transverse shear stress $\bar{\sigma}_{xz}$ are reported in Fig. 8. In all cases, selectively integrated (IS) Q9 elements have been employed for the thin plate ($S = 100$). A linear convergence rate can be recognized for both stress components, in accordance with the

quadratic rate of the displacement observed in Fig. 7(c). It is to note that the error in the stresses is always larger than the one in the displacements, and that the computation of σ_{xx} is more accurate than that of σ_{xz} . Moreover, it is interesting to observe that the convergence lines of all the selected formulations are identical.

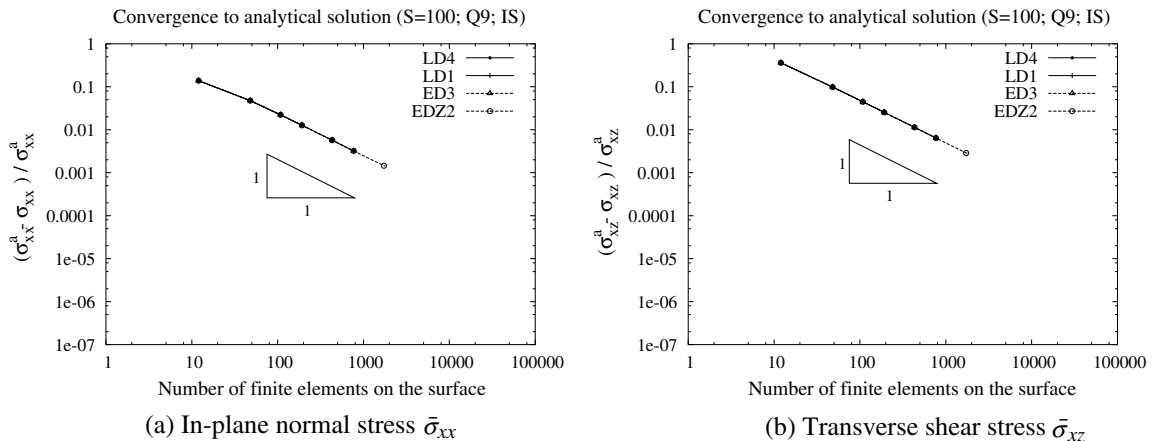


Fig. 8. Convergence analysis: stresses for $S = 100$, IS.

5.2. Assessment of plate theories

This section is devoted to a brief comparison of the present FE with the exact elasticity results reported by Pagano [31]. For the sake of completeness, the analytical closed-form solution as well as the exact 3D solution of Pagano for the selected quantities given in Eq. (28d) have been reported in Tables 1 and 2. All presented results are referred to both a thin ($S = 100$) and a thick ($S = 4$) plate. Table 3 compares the transverse displacement \bar{w} of the 3D solution of Pagano with those obtained with the considered formulations for both the FEM and the closed-form solution technique. The convergence to the exact solution is visualized in Fig. 9. The values in parentheses represent the values obtained with the analytical solution method for the correspondent thickness assumption. It can be clearly seen that the FE solution converges to the corresponding analytical solution, rather than to the 3D elasticity solution. Thus, the error introduced by the FE approximation is shown to vanish. The difference between the analytical solution or, equivalently, the converged FE solution, and the exact solution is a measure of the error introduced by the thickness assumptions. As usually occurs

Table 3

Normalized transverse deflection \bar{w} in the plate center

3D exact	$S = 100, 0.508$		$S = 4, 2.82$	
	FEM (IS)	Closed-form	FEM (IN)	Closed-form
LD4	0.50766	0.50766	2.82111	2.82112
LD3	0.50766	0.50766	2.82100	2.82101
LD2	0.50766	0.50766	2.79832	2.79831
LD1	0.50719	0.50719	2.72085	2.72085
ED4	0.50708	0.50708	2.62471	2.62471
ED3	0.50708	0.50708	2.62671	2.62671
ED2	0.50588	0.50588	2.03520	2.03520
ED1	0.50335	0.50335	2.05112	2.05112

Thick ($S = 4$) and thin ($S = 100$) plate; Q9 elements; converged FE solutions.

for two-dimensional models, this error is larger in the case of a thick plate, see Fig. 9(a) and (b).

The hierarchic nature of the presented formulations becomes evident observing that layerwise, higher-order formulations are generally more accurate than lower-order, ESL formulations. The introduction of the MZZF can noticeably improve the result: in the present case study, the EDZ3 formulation recovers the LD4 model for both

Table 1

Closed-form solutions for all formulations compared to exact elasticity solution and CLT solution given by Pagano in Ref. [31]

$S = 4$	\bar{w}	$\bar{\sigma}_{xx}$	$\bar{\sigma}_{yy}$	$\bar{\sigma}_{xy}$	$\bar{\sigma}_{xz}$	$\bar{\sigma}_{yz}$
Exact	2.82	1.14	-0.119	0.0281	0.351	0.0334
LD4	2.82	1.14	-0.119	0.0281	0.351	0.0334
LD3	2.82	1.14	-0.119	0.0281	0.351	0.0334
LD2	2.80	1.13	-0.118	0.0278	0.347	0.0332
LD1	2.72	1.01	-0.111	0.0264	0.352	0.0321
EDZ3	2.81	1.17	-0.084	0.0280	0.347	0.0330
EDZ2	2.72	1.02	-0.094	0.0260	0.352	0.0322
EDZ1	2.74	0.98	-0.098	0.0270	0.312	0.0352
ED4	2.63	1.11	-0.111	0.0266	0.376	0.0322
ED3	2.63	1.11	-0.110	0.0266	0.376	0.0321
ED2	2.04	0.64	-0.090	0.0189	0.436	0.0271
ED1	2.05	0.61	-0.089	0.0195	0.436	0.0262
CLT	0.503	0.623	-0.0252	0.0083	0.440	0.0108

Thick plate ($S = 4$).

Table 2

Closed-form solutions for all formulations compared to exact elasticity solution and CLT solution given by Pagano in Ref. [31]

$S = 100$	\bar{w}	$\bar{\sigma}_{xx}$	$\bar{\sigma}_{yy}$	$\bar{\sigma}_{xy}$	$\bar{\sigma}_{xz}$	$\bar{\sigma}_{yz}$
Exact	0.508	0.624	-0.0253	0.0083	0.439	0.0108
LD4	0.508	0.624	-0.0253	0.0083	0.439	0.0108
LD3	0.508	0.624	-0.0253	0.0083	0.439	0.0108
LD2	0.508	0.624	-0.0253	0.0083	0.439	0.0108
LD1	0.507	0.625	-0.0261	0.0083	0.439	0.0108
EDZ3	0.508	0.624	-0.0251	0.0083	0.439	0.0108
EDZ2	0.507	0.624	-0.0251	0.0083	0.439	0.0108
EDZ1	0.505	0.624	-0.0260	0.0083	0.439	0.0114
ED4	0.507	0.624	-0.0251	0.0083	0.439	0.0108
ED3	0.507	0.624	-0.0252	0.0083	0.439	0.0108
ED2	0.506	0.623	-0.0251	0.0083	0.440	0.0108
ED1	0.503	0.623	-0.0259	0.0083	0.439	0.0113
CLT	0.503	0.623	-0.0252	0.0083	0.440	0.0108

Thin plate ($S = 100$).

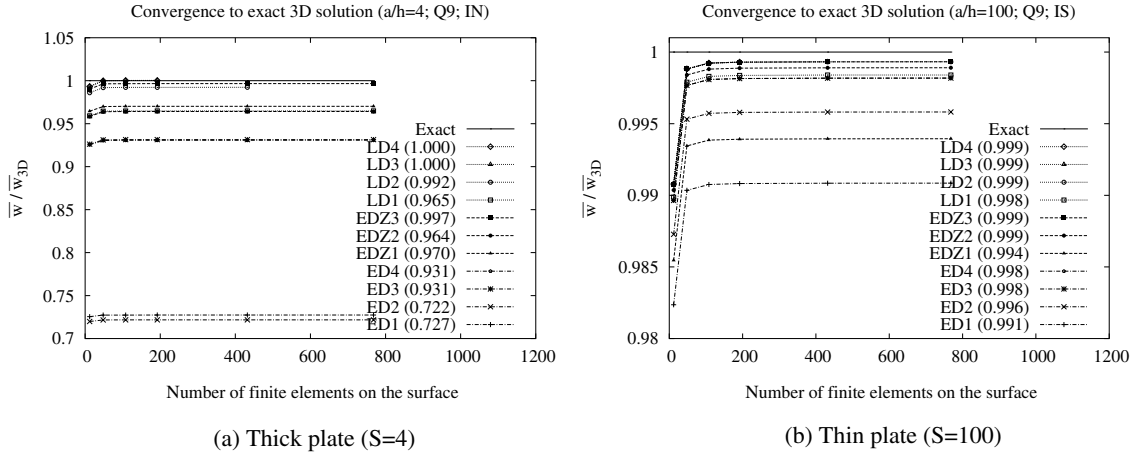


Fig. 9. Convergence to the exact 3D solution: normalized transverse deflection \bar{w} .

thin and thick plates. In order to complete this qualitative assessment, the convergence behavior of the stress components σ_{xx} and σ_{xz} with respect to the exact solution are given in Fig. 10 for both the thick and thin plate. Again, the values in parentheses indicate the values obtained by the closed-form solution. The stresses show the same

behavior of the displacements, i.e. they converge to the analytical solution σ^a . All the selected formulations except LD4 have the same number of terms for the thickness expansions: LD1, EDZ2 and ED3 employ four DOFs for representing the thickness behavior. In all cases, recalling also the results in Figs. 7 and 8, it has to be noticed that

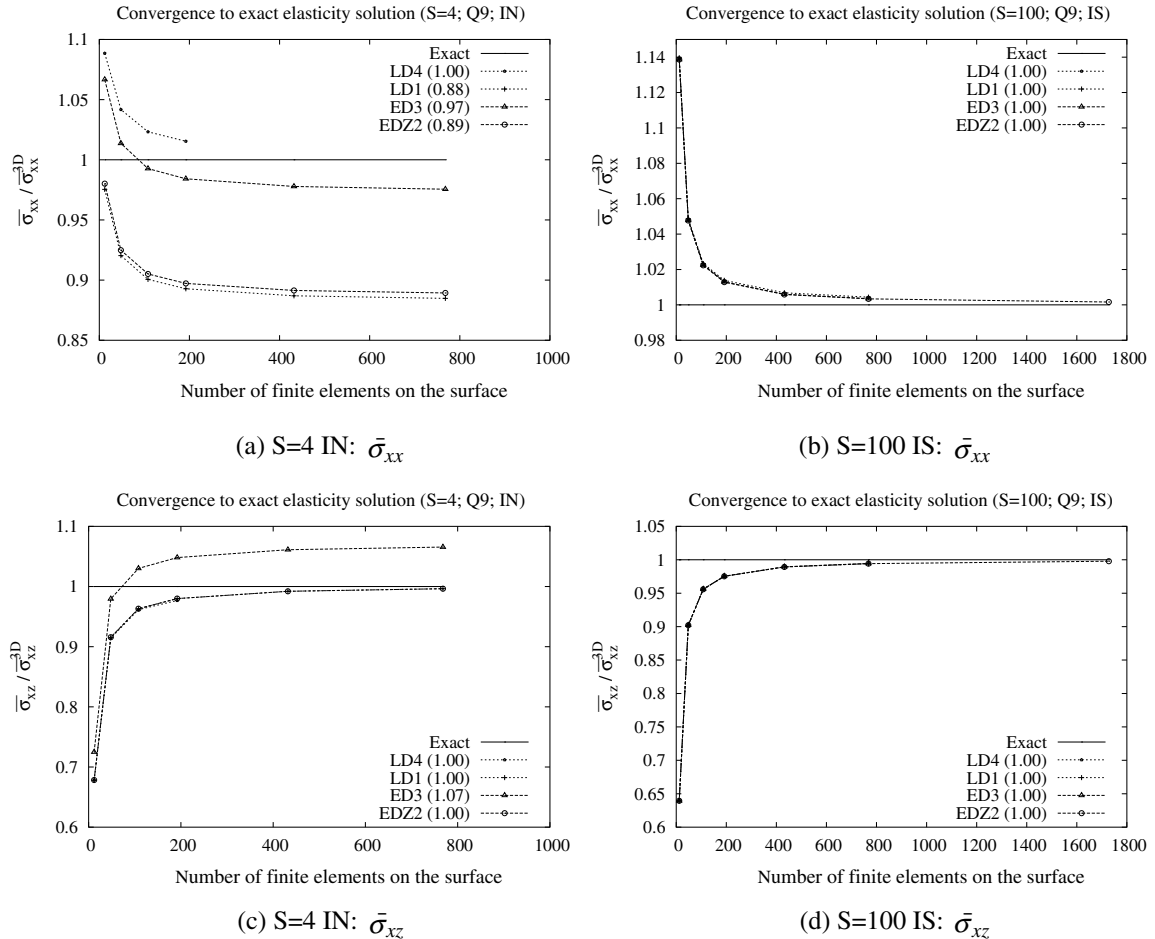


Fig. 10. Convergence to the exact 3D solution: normalized stresses $\bar{\sigma}_{xx}$ and $\bar{\sigma}_{xz}$.

the number of nodal unknowns, i.e. the employed order of expansion, does not influence the numerics of the finite element approximation, except for the already mentioned *shear locking* phenomenon. Observing Fig. 10(a) and (b), it is seen that the FE solution for the in-plane stress σ_{xx} tends asymptotically to the analytical solution from above, whereas the transverse shear stress converges to its asymptotic value σ_{xz}^a starting from smaller values (Fig. 10(c) and (d)).

A remarkable difference between the convergence behavior of the displacements (Fig. 9) and the one of the stresses (Fig. 10) consists in the fact that, in the latter case, for coarse meshes the solution of lower-order formulations (e.g. ED3) may be more accurate than e.g. LD4 formulations; this occurs whenever the convergence curve of the FE solution crosses the exact solution line and this fact arises only in the computation of the stresses with lower-order formulations (e.g. ED3 in Fig. 10(a) and (c)). These effects are in general due to the superimposition of two distinct error sources: on the one hand the error introduced by the thickness assumptions, on the other hand the error introduced by the crude finite element approximation. In the case of the computation of stresses with the ED3 formulation, these two errors cancel out each other yielding a very accurate result for coarse discretizations.

5.2.1. Considerations on thickness locking

In the selected case study, no thickness locking effects could be recognized. This spurious phenomenon is introduced by the three-dimensional constitutive equations for the description of a shell or plate element involving the same assumptions for all displacement terms. It is due to the coupling via the Poisson effect of the transverse normal stress $\sigma_{zz}(z)$ with the in-plane direct strains. If assumptions of the same order are chosen for both the in-plane displacements u , v and the transverse deflection w , the resulting distribution of $\sigma_{zz}(z)$ does in fact not match the distribution of the conjugated strain $\epsilon_{zz} = w_{,z}$. A detailed reference on this subject is provided by, e.g., the work of Bischoff and Ramm [33].

In the following, some considerations are made to explain why thickness locking has not been found in the numerical assessment given in this work. First, thickness locking is expected to have heavier consequences within first-order formulations compared to higher-order ones. In fact, the inconsistency between the linear transverse stress distribution and a constant transverse strain distribution in the thickness direction is supposed to be more severe than the one caused by a mismatch of distributions involving higher-order terms. Therefore, the only formulations which could have shown some Poisson locking effects are the first-order ED1, EDZ1 and LD1. Finally, since the error is proportional to the material coefficient which is responsible for the coupling between the in-plane and the transverse behavior, and due to the high E_I/E_T ratio of the employed Gr/Ep material, the thickness locking is definitively less pronounced in comparison to, e.g., isotro-

pic materials. Therefore, it can be stated that the thickness locking problem occurring in UF-based elements should be addressed in future by accounting for curvature effects and more severe material properties.

6. Conclusions

This paper has presented a class of two-dimensional finite plate elements based on the Unified Formulation proposed by Carrera for an accurate analysis of laminated structures. The Unified Formulation allows an implementation-friendly, hierarchic modeling of multilayered plates and shells. In order to reach a high accuracy even in the computation of thick components, the transverse normal stress is normally retained in the arising formulations. For the first time, an assessment has been proposed of the numerical properties of finite elements based on the Unified Formulation. The spurious stiffening effect characterizing the global behavior of this class of elements at small thickness ratios turned out to be the well-known *shear locking* effect. Therefore, classical procedures aimed at the control of this spurious effect can be successfully implemented. In this work, the selectively reduced integration procedure has been considered. A numerical assessment of the convergence rates and of the convergence behavior has been presented: the elements are robust and recover the analytical solutions in case of both thick and thin plates. For the sake of completeness, some comments regarding the thickness locking effect have been made. The present work gains particular importance in view of an implementation of these elements in commercially available FE-packages.

References

- [1] Ambartsumian SA. Contributions to the theory of anisotropic layered shells. *Appl Mech Rev* 1962;15:249–345.
- [2] Noor AK, Burton WS. Assessment of computational models for multilayered shells. *Appl Mech Rev* 1990;43(4):67–97.
- [3] Carrera E. Theories and finite elements for multilayered, anisotropic, composite plates and shells. *Arch Comput Meth Eng* 2002;9(2): 87–140.
- [4] Librescu L. *Elasto-statics and kinetics of anisotropic and heterogeneous shell-type structures*. Leyden, Netherland: Noordhoff Int.; 1975.
- [5] Kant T, Swaminathan K. Estimation of transverse/interlaminar stresses in laminated composites – a selective review and survey of current developments. *Compos Struct* 2000;49:65–75.
- [6] Chang F-K, Chang K-Y. A progressive damage model for laminated composites containing stress concentrations. *J Compos Mater* 1987; 21:834–55.
- [7] Carrera E. C_2^0 -Requirements – models for the two-dimensional analysis of multilayered structures. *Compos Struct* 1997;37:373–83.
- [8] Koiter WT. A consistent first approximation in the general theory of thin elastic shells. In: Koiter WT, editor. *The theory of thin elastic shells*. IUTAM. Delft: North-Holland; 1959. p. 12–33.
- [9] Carrera E. An assessment of mixed and classical theories for thermal stress analysis. *J Therm Stresses* 2000;23:797–831.
- [10] Meyer-Piening H-R. Experiences with ‘exact’ linear sandwich beam and plate analyses regarding bending, instability and frequency

- investigations. Proceedings of the fifth international conference on sandwich constructions. Zurich, Switzerland: EMAS Publication; 2000. p. 37–48.
- [11] Reissner E. On a mixed variational theorem and on a shear deformable plate theory. *Int J Numer Meth Eng* 1986;23:193–8.
- [12] Toledano A, Murakami H. A high-order laminated plate theory with improved in-plane responses. *Int J Solids Struct* 1987;23:111–31.
- [13] Carrera E. Developments, ideas and evaluations based upon Reissner's mixed variational theorem in the modeling of multilayered plates and shells. *Appl Mech Rev* 2001;54(4):301–29.
- [14] Reddy JN. *Mechanics of laminated composite plates and shells: theory and analysis*. Boca Raton: CRC Press; 2004.
- [15] Carrera E. Theories and finite elements for multilayered plates and shells: A unified compact formulation with numerical assessment and benchmarking. *Arch Comput Meth Eng* 2003;10(3):215–96.
- [16] Reddy JN. On refined computational models of composite laminates. *Int J Numer Meth Eng* 1989;27:361–82.
- [17] Bathe KJ, Dvorkin EN. A four node plate bending element based on Mindlin/Reissner plate theory and mixed interpolation. *Int J Numer Meth Eng* 1985;21:367–83.
- [18] Simo JC, Rifai S. A class of mixed assumed strain methods and the method of incompatible modes. *Int J Numer Meth Eng* 1990;29:1595–638.
- [19] Ausserer MF, Lee SW. An eighteen-node solid element for thin shell analysis. *Int J Numer Meth Eng* 1988;26:1345–64.
- [20] Kulikov GM, Plotnikova SV. Non-linear strain-displacement equations exactly representing large rigid-body motions. Part 1: Timoshenko–Mindlin shell theory. *Comput Meth Appl Mech Eng* 2003;192:851–75.
- [21] Büchter N, Ramm E, Roehl D. Three-dimensional extension of nonlinear shell formulation based on the enhanced assumed strain concept. *Int J Numer Meth Eng* 1994;37:2551–68.
- [22] Parisch H. A continuum-based shell theory for non-linear applications. *Int J Numer Meth Eng* 1995;38:1855–83.
- [23] Yang HT, Saigal S, Masud A, Kapania RK. A survey of recent shell finite elements. *Int J Numer Meth Eng* 2000;47:101–27.
- [24] Carrera E, Demasi L. Classical and advanced multilayered plate elements based upon PVD and RMVT. Part 2: Numerical implementations. *Int J Numer Meth Eng* 2002;55:253–91.
- [25] Washizu K. *Variational methods in elasticity and plasticity*. 2nd ed. Oxford, UK: Pergamon Press; 1975.
- [26] Jones RM. *Mechanics of composite materials*. McGraw-Hill; 1975.
- [27] Carrera E. A class of two-dimensional theories for multilayered plates analysis. *Atti Acc Sci Torino, Mem Sci Fis* 1995;19–20:49–87.
- [28] Murakami H. Laminated composite plate theory with improved in-plane response. *J Appl Mech* 1986;53:661–6.
- [29] Carrera E. On the use of Murakami's zig-zag function in the modeling of layered plates and shells. *Comput Struct* 2004;82:541–54.
- [30] Carrera E, Demasi L. Classical and advanced multilayered plate elements based upon PVD and RMVT. Part 1: Derivation of finite element matrices. *Int J Numer Meth Eng* 2002;55:191–231.
- [31] Pagano NJ. Exact solutions for rectangular bidirectional composites and sandwich plates. *J Compos Mater* 1970;4:20–34.
- [32] Carrera E. Evaluation of layerwise mixed theories for laminated plates analysis. *AIAA J* 1998;36(5):830–9.
- [33] Bischoff M, Ramm E. On the physical significance of higher-order kinematic and static variables in a three-dimensional shell formulation. *Int J Solids Struct* 2000;37:6933–60.